Reaction Distribution with Time in Fuel Cells using a Terahertz Chemical Microscope

Tetsuya Kusaka, Kazuki Koiso, Kenji Sakai, Toshihiko Kiwa, and Keiji Tsukada
Graduate School of Natural Science and Technology,
Okayama University,
Okayama, Japan
E-mail: (pkta5jir, p4jh6yr8)@s.okayama-u.ac.jp
(sakai-k, kiwa, tsukada)@okayama-u.ac.jp

***Abstract*—The visual evaluation of fuel cells by conventional means is impossible. To improve the power generation efficiency of fuels cells, the evaluation of catalytic reactions on the electrodes and ion propagation in the electrolyte are important. We developed a terahertz chemical microscope (TCM) to visualize the electric potential shift in the catalytic electrodes of fuel cells. The potential energy shift of the fuel cells due to the dissociation of gases was visualized using TCM during fuel cell operation.**

Keywords–TCM; THz; fuel cell; evaluation

I. INTRODUCTION

Energy and environmental issues have recently become crucial and require energy solutions of high efficiency and low environmental load. Thus, the use of hydrogen gas has attracted attention. Fuel cells are high-efficiency devices that transform chemical energy to electric energy. However, the power generation efficiency of fuel cells has to improve. Hence, evaluation methods and investigation of the catalytic reactions on the catalytic electrodes and ion propagation in the electrolyte are required.

Recently, we have developed a terahertz chemical microscope (TCM) to evaluate the distribution of the electric potential on a semiconductor-based device referred to as THz sensing plate. Terahertz (THz) waves radiating from the THz sensing plate can be related to the electric potential at the surface of the THz sensing plate [1]–[4].

Conventional evaluation methods of surfaces are atomic force microscopy [5], scanning electron microscopy [6], and transmission electron microscopy. Kelvin probe microscopy (KPM) can measure the electric potential distribution on the electrode surface [7]. However, KPM probe needs to closely touch the electrode surface; thus, in general, it is difficult for KPM to measure the electric potential while the fuel cell is in operation. On the other hand, the TCM can measure the electric potential of catalytic metals without coming to contact with the surface of metals.

In a previous study, the time variation of the THz signal during the fuel cell operation was measured [8], and the signal was observed to drift due to the diffusion of protons in the proton membrane. In this study, the two-dimensional imaging of the THz signal during the long operation of fuel cells is demonstrated, and the potential distribution on the electrodes is discussed.

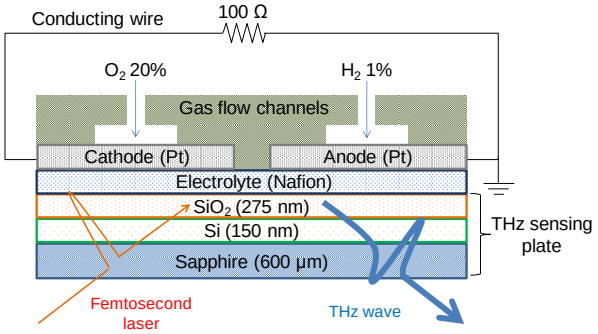

Figure 1. Schematic diagram of a fuel cell fabricated on the THz sensing plate.

II. EXPERIMENTS

Figure 1 shows the schematic diagram of the fuel cell on the THz sensing plate. The sensing plate consists of SiO_2 (275 nm) and Si (150 nm) layers on a sapphire substrate (600 μm). Because of its excellent mechanical and thermal stability, Nafion® (10%) membrane was applied on the surface of the SiO_2 layer by spin coating and baked for 90 s at 90 °C. Platinum (Pt) was deposited on the Nafion membrane to serve as catalytic metal electrodes by conventional sputtering techniques. Before the experiments, we confirmed that the fuel cell fabricated on the THz sensing plate generated voltage as well as the actual fuel cells.

Figure 2 shows the energy band diagram of the sensing plates, on which the Nafion membrane and the Pt thin film were fabricated. When femtosecond laser pulses were

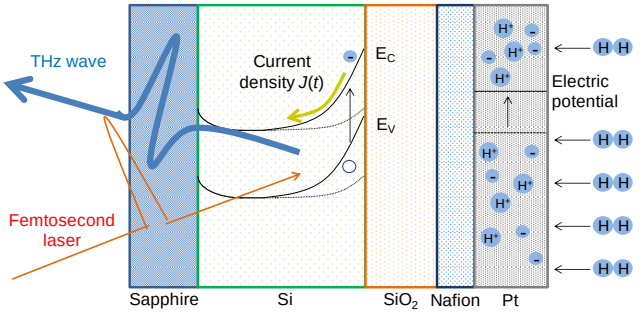

Figure 2. Energy band diagram of the THz sensing plates. E_C is the conduction band and E_V is the valence band.

 ISBN: 978-1-61208-375-9

irradiated from the sapphire side of the THz sensing plate, photoexcited carriers were generated in the Si layer. The photoexcited carriers were accelerated by the electric field generated by the depletion layer, and THz waves were radiated to free space.

The relation between the radiated THz waves and the electric potential on the THz sensing plate is described with following equation:

$$E_{\mathrm{THz}} \propto \frac{\partial J(t)}{\partial t} \propto e\frac{\partial n(t)}{\partial t}v(t) + en(t)\frac{\partial v(t)}{\partial t}, \qquad (1)$$

where $J(t)$ is the current density, e is the elementary charge, $n(t)$ is the excitation carrier density, and $v(t)$ is the carrier velocity. Hydrogen molecules are dissociated when hydrogen gas is exposed to the Pt electrodes. The hydrogen ions (H^+) diffuse into the Pt electrodes and then the Nafion membrane. The H^+ ions are adsorbed on the SiO_2 surface of the THz sensing plate. The carrier acceleration in the second term of (1) is equal to the local electric field E_{local} in the sensing plate; therefore, the amplitude of the THz wave emitted from the THz sensing plate is proportional to the local electric field.

The amplitude of the radiated THz wave is

$$E_{\mathrm{THz}} \propto E_{\mathrm{local}} = \sqrt{eN_{\mathrm{D}}/2\varepsilon} \times \sqrt{\phi}, \qquad (2)$$

where E_{local} is the local electric field, N_{D} is the carrier density of the Si surface, ε is the dielectric constant of Si, and ϕ is the electric potential. The shift in the electric potential of Pt due to the reaction of hydrogen gas is expressed by using the Nernst equation:

$$\phi = const - (RT/zF) \ln P_{\mathrm{H_2}}, \qquad (3)$$

where F is the Faraday constant, z is the number of electrons transferred in the cell reaction, R is the gas constant, T is the absolute temperature, and P_{H2} is the partial pressure of hydrogen. Equation (3) shows that the electric potential of the THz sensing plate shifts because of the adsorption of hydrogen gas to the Pt electrodes in the fuel cell. The visualization of the chemical reactions can be achieved by scanning the irradiation point of the femtosecond laser because the radiated THz wave depends on the local electric field of the depletion layer where the laser is irradiated. In the fuel cell, the chemical reaction at the anode and the cathode of the operating fuel cell can be expressed as follows:

$$\text{Anode: } H_2 \rightarrow 2H^+ + 2e^- \qquad (4)$$

$$\text{Cathode: } 2H^+ + 1/2O_2 + 2e^- \rightarrow H_2O. \qquad (5)$$

The electric potential shift because of the adsorption of hydrogen gas in the anode is obtained as the amplitude of the radiated THz wave by (3). At the anode, the hydrogen molecules, which reach Pt, dissociate to H^+ and electrons. H^+ reaches the cathode through the Nafion membrane. The electrons move to the cathode along the conducting wire. The THz amplitude from the anode increases with increasing electric potential because of the reduction of hydrogen. On the other hand, the amplitude of the radiated THz wave decreases due to the oxidation reaction of H^+ in the cathode.

Figure 3 shows the optical setup of TCM. The fuel cell fabricated on the THz sensing plate is fixed on the X–Y stage to scan the femtosecond laser. Before irradiating the THz sensing plate, the femtosecond laser pulses pass through the condensing lens to increase the spatial resolution. The Ti:sapphire laser is a femtosecond laser with a central wavelength of 780 nm, a pulse width of 100 fs, and a repetition frequency of 82 MHz. A conventional photoconductive antenna was used to detect the radiated THz waves whose amplitudes are related to the electric potential of the THz sensing plate. Figure 4 shows a photograph of

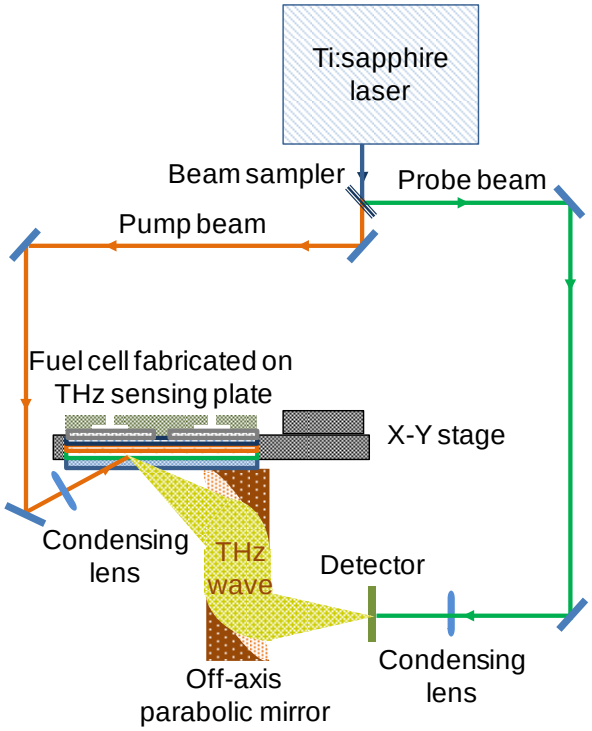

Figure 3. Setup of TCM.

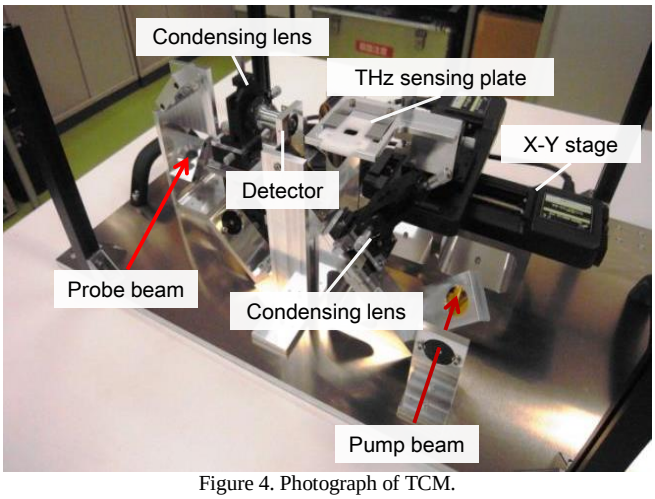

Figure 4. Photograph of TCM.

TCM. All optical components were attached on the same platform sterically. The area of the platform is 628 × 379 mm^2.

III. RESULTS

Figure 5 shows the time variation of the distribution of the radiated THz amplitude from the THz sensing plate. The areas surrounded by the blue line show the catalytic electrodes. Hydrogen gas (1%) and oxygen gas (20%) in the nitrogen gas were, respectively, introduced to the anode and cathode to operate the fuel cell. Figures 5 (a), (b), and (c) show the change in the THz amplitude distribution obtained (a) before and after power generation for 1 h, (b) between 1–2 h, and (c) between 2–3 h. Initially, the THz amplitude at the cathode decreases, whereas the THz amplitude at the anode increases. The change in the THz signals was larger in magnitude at the upper parts of the electrodes. Subsequently, the THz amplitude was saturated across the electrodes.

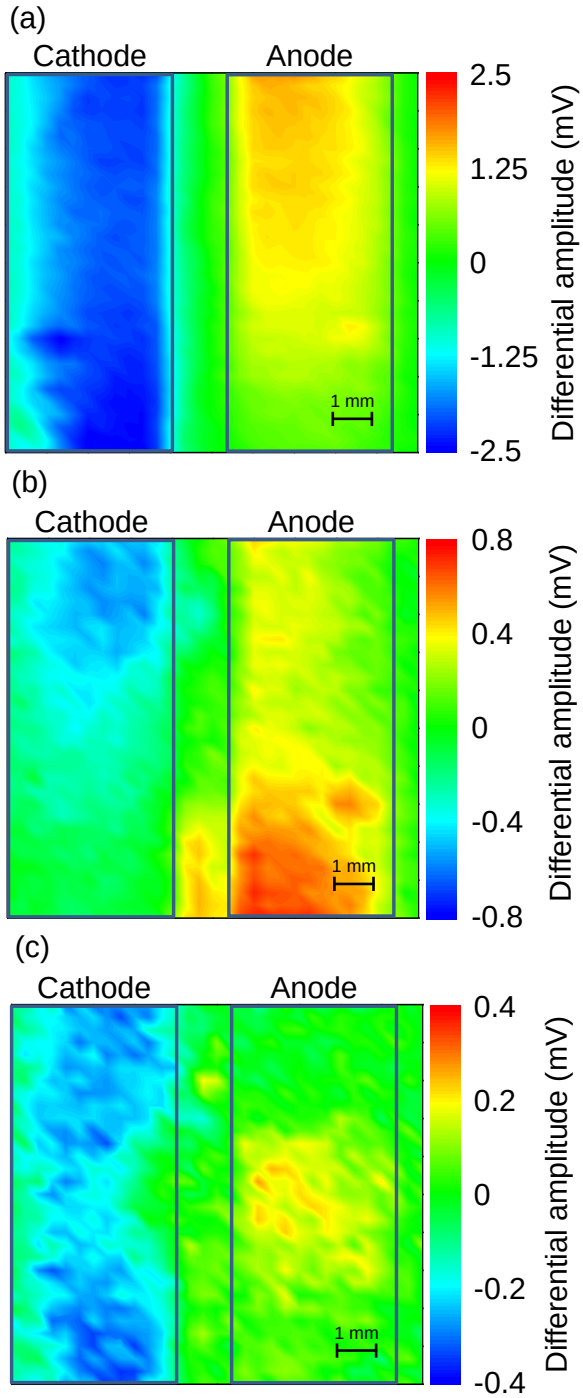

Figure 5. Variation of the THz amplitude distribution obtained after power generation (a) for 1 h, (b) between 1–2 h, and (c) between 2–3 h.

The average values of the radiated THz amplitude from the anode and the cathode during the fuel cell operation are plotted in Figure 6. The electric potential in the anode increases, whereas that in the cathode decreases and, subsequently, both become saturated. This shows that TCM can measure the reaction amount in the catalytic electrodes.

IV. CONCLUSION AND FUTURE WORK

We mapped the radiated THz waves from a THz sensing plate, on which a fuel cell was fabricated, during fuel cell operation. The THz amplitude at the anode increased, whereas that at the cathode decreased. The nonuniformity of the THz amplitude can be seen at the anode and cathode. The results agree with past experiments. We also confirmed the reaction distribution in the catalytic electrodes with time, which shows that TCM can measure the reaction distribution in the catalytic electrodes. The radiated THz amplitude from the anode and cathode reach saturation with time. Evidently, TCM can measure the reaction amount in the catalytic metal electrodes. In conclusion, we showed that TCM can be used to evaluate fuel cells. When TCM is commercialized, we will be able to visually evaluate the uniformity of the electrolyte and electrodes. We conducted the experiments using only Nafion 10%; thus, we plan to measure the performance of fuel cells using Nafion with different concentrations or other electrolytes. The relation between TCM images and fuel cell efficiency is presently under investigation.

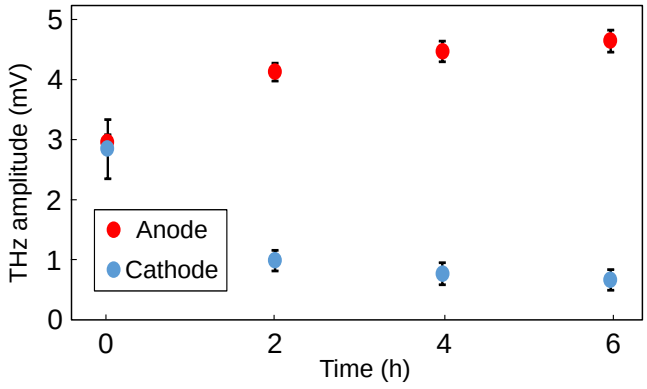

Figure 6. Time variation of the radiated THz amplitude due to the voltage generation in the fuel cell.

 ISBN: 978-1-61208-375-9

ACKNOWLEDGMENT

This study was partially supported by the Japan Science and Technology Agency.

REFERENCES

[1] T. Kiwa, J. Kondo, S. Oka, I. Kawayama, H. Yamada, M. Tonouchi, and K. Tsukada, "Chemical sensing plate with a laser-terahertz monitoring system," Appl. Optics, 47, 18, pp. 3324–3327, 2008.

[2] T. Kiwa, S. Oka, J. Kondo, I. Kawayama, H. Yamada, M. Tonouchi, and K. Tsukada, "A terahertz chemical microscope to visualize chemical concentration in microfluidic chips," Jpn. J. Appl. Phys., 46, 41–44, pp. L1052–L1054, 2007.

[3] T. Kiwa, K. Tsukada, M. Suzuki, M. Tonouchi, S. Migitaka, and K. Yokosawa, "Laser terahertz emission system to investigate hydrogen gas sensors," Appl. Phys. Lett., 86, 261102, 2005.

[4] T. Kiwa, T. Hagiwara, M. Shinomiya, K. Sakai, and K. Tsukada, "Work function shifts of catalytic metals under hydrogen gas visualized by terahertz chemical microscopy," Opt. Express, 20, 11637–1164, 2012.

[5] H. Ghassemi, J. E. McGrath, and T. A. Zawodzinski Jr, "Multiblock sulfonated–fluorinated poly (arylene ether) s for a proton exchange membrane fuel cell," Polymer, 47, 4132–4139, 2006.

[6] J. Xie, D. L. Wood, K. L. More, P. Atanassov, and R. L. Borup, "Microstructural changes of membrane electrode assemblies during PEFC durability testing at high humidity conditions," J. Electrochem. Soc., 152, A1011–A1020, 2005.

[7] J. Zhang, G. Yin, and Z. Wang, and Y. Shao, "Effects of MEA preparation on the performance of a direct methanol fuel cell," J. Power Sources 160, 1035–1040, 2006.

[8] T. Kusaka, K. Koiso, K. Sakai, T. Kiwa, and K. Tsukada "Catalytic reactions of the fuel cells visualized by THz chemical microscope," In Laser Applications to Chemical, Security and Environmental Analysis (pp. LTu3D-6). Optical Society of America, 2014.

 ISBN: 978-1-61208-375-9